LANGMUIR

Article

Atomic Layer Deposition for Coating of High Aspect Ratio TiO2 Nanotube Layers

Raul Zazpe, Martin Knaut, Hanna Ingrid Sopha, Ludek Hromadko, Matthias Albert, Jan Prikryl, Viera Gartnerova, Johann W. Bartha, and Jan M. Macak

Langmuir, **Just Accepted Manuscript** • DOI: 10.1021/acs.langmuir.6b03119 • Publication Date (Web): 19 Sep 2016

ACS Publications

Langmuir is published by the American Chemical Society. 1155 Sixteenth Street N.W., Washington, DC 20036

Atomic Layer Deposition for Coating of High Aspect Ratio TiO_2 Nanotube Layers

Raul Zazpe[†], Martin Knaut[‡], Hanna Sopha[†], Ludek Hromadko[†], Matthias Albert[‡], Jan Prikryl[†], V. Gärtnerová[§], Johann W. Bartha[‡], and Jan M. Macak[†]*

[†]Center of Materials and Nanotechnologies, Faculty of Chemical Technology, University of Pardubice, Nam. Cs. Legii 565, 53002 Pardubice, Czech Republic.

[‡]Institute of Semiconductors and Microsystems and Center for Advancing Electronics Dresden (cfaed), Noethnitzer Str. 64, Technische Universität Dresden, 01062 Dresden, Germany

[§] Laboratory of Nanostructures and Nanomaterials, Institute of Physics of the CAS, v.v.i., Na Slovance 2, 182 21 Prague 8, Czech Republic

Keywords: TiO_2, nanotubes, coating, ALD, diffusion

We present an optimized approach for the deposition of Al_2O_3 (as a model secondary material) coating into a high aspect ratio (≈180) anodic TiO_2 nanotube layers using atomic layer deposition (ALD) process. In order to study the influence of the diffusion of the Al_2O_3 precursors on the resulting coating thickness, ALD processes with different exposure times (i.e. 0.5, 2, 5 and 10 sec) of the trimethylaluminium (TMA) precursor were performed. Uniform coating of the nanotube interiors was achieved with longer exposure times (5 and 10 sec), as verified by

detailed scanning electron microscopy analysis. Quartz crystal microbalance measurements were used to monitor the deposition process and its particular features due to the tube diameter gradient. Finally, theoretical calculations were performed to calculate the minimum precursor exposure time to attain uniform coating. Theoretical values on the diffusion regime matched with the experimental results and helped to obtain valuable information for further optimization of ALD coating processes. The presented approach provides a straightforward solution towards the development of many novel devices, based on a high surface area interface between TiO_2 nanotubes and a secondary material (such as Al_2O_3).

Introduction

Over the past 20 years, self-organized valve metal oxide nanoporous or nanotubular structures have attracted huge scientific and technological attention, due to their unique architecture and intriguing properties. In particular, this accounts for nanoporous anodic alumina,[1,2] and nanotubular anodic titania[3-6] prepared by a low-cost electrochemical anodization of corresponding metal substrates. Nanoporous alumina, typically in the form of membranes, has been mainly employed as the templating or supporting material for synthesis of various functional materials and devices.[7-12] In contrast to nanoporous alumina, TiO_2 nanotube layers have been exploited for a significantly larger number of applications, owing to the semiconductive nature of TiO_2, unique tubular architecture, and chemical stability. Outstanding performance of TiO_2 nanotubes was revealed mainly in photocatalysis, solar cells, self-cleaning, and biomedical fields[13-15] among others. Significant and valuable efforts were carried out to tune the aspect ratio of the nanotubes,[5,6,16-18] to improve the tube ordering,[19-24] crystallinity,[25-29] and to prepare tube layers on various substrates, including conductive glasses[30-32] for various functional devices. On the other hand, comparably smaller efforts were devoted to obtain a uniform coating

of the tubes with a secondary material, such as metals, oxides (incl. those with semiconducting properties), quantum dot materials, conducting polymers, or chalcogenides. Until now, numerous deposition approaches were reported to coat or fill the interior parts of the nanotubes, including electrodeposition,[33-36] chemical bath deposition,[37-40] spincoating,[41,42] sputtering[43-45] and atomic layer deposition (ALD). While ALD is one of the most promising deposition techniques for its excellent homogeneity and thickness accuracy, there have been only few reports published employing this technique for an introduction of the secondary material in the nanotube layers.[46-53] In particular, ALD has recently been reported for the deposition of Al_2O_3, as secondary material, onto TiO_2 nanotubular structures for enhanced water splitting[52] and more efficient dye sensitized solar cells.[53] The Al_2O_3 coating resulted in an improvement of the electrochemical and photovoltaic performance displayed, both ascribed to the passivation of the surface states that leads to a reduction of the electron-hole recombination rate at the surface of the TiO_2 nanotube layer electrode. On the other hand, these two reports[52-53] did neither provide any information about the influence of ALD parameters (especially precursor diffusion times) on the overall coating, nor contained any quartz crystal microbalance data. Nevertheless, these publications confirm that an introduction of the secondary material in the nanotubes, by a very uniform and precisely controllable deposition process, results in many advanced functionalities of the newly prepared composite TiO_2-based nanotube layers, similarly as it did for nanoporous materials.[54,55] This can be especially true for high aspect ratio TiO_2 nanotube layers that are even more promising for applications than their lower aspect ratio counterparts.[13-15] However, coating of high aspect ratio nanostructures is a relatively time consuming and demanding in terms of precursor doses.[54,56] Thus, to avoid unnecessarily long processes and consumption of expensive precursor(s), the optimization of the ALD coating of high aspect ratio TiO_2 nanotube layers with

secondary materials is highly demanded. It was only recently shown by Macak et al. that nanotube layers with aspect ratio of ≈ 80 can obtain a uniform In_2O_3 coating along the interiors of TiO_2 nanotube layers resulting in significantly enhanced antireflection performance.[51] However, the diffusion of the precursors was far from being optimized and the resulting coating had unequal thickness along the tube walls. Nevertheless, this paper indicated, how crucial is to enable within the ALD process the proper diffusion of the precursors inside the nanotubes to achieve the same coating thickness throughout the whole nanotube layer.

Thus, in the present work, a detailed study on the deposition process to achieve a uniform coating of very high aspect ratio TiO_2 nanotube layers (≈180) with a secondary material by ALD is reported for the first time including detailed SEM analyses of the coatings. The aspect ratio in this work is considered as the ratio between the nanotube layer thickness (20 μm) and the average tube diameter (110 nm) at the top of the nanotube layer. Thus it accounts for approximately 180. As a model secondary material, aluminum oxide (Al_2O_3) was deposited from trimethyl-aluminium (TMA) and water precursors. To study the influence of the TMA diffusion time on the thickness of the Al_2O_3 coating along the walls of TiO_2 nanotubes, different TMA exposure times during the process were employed. A thorough scanning electron microscopy (SEM) analysis was employed to evaluate the coating thickness of the interior nanotube surface at different depth levels inside the nanotube layer: top, near top, center and bottom. In addition, quartz crystal microbalances (QCM) with attached TNT membranes were employed to monitor the ALD process in the TNTs. This novel approach enables essentially a more detailed understanding of the applied coating process and provides new insights in the demands and challenges of ALD coating of high aspect ratio nanostructures. Finally, theoretical minimum

TMA precursor exposure time was calculated in order to get a deeper insight on the deposition process of a secondary material inside the tubes.

Experimental Section

The TiO_2 nanotube layers, with a thickness of ~20 μm and a nanotube diameter of ~110 nm (AR ≈180), were prepared by anodization of Ti foils (Sigma-Aldrich, 0.127 mm thick, 99.7 % purity) at 60 V for 4 h (the sweep rate was 1 V/s). Prior to the anodization the Ti foils were degreased by sonication in isopropanol and acetone, then rinsed with isopropanol and dried in air. The anodization itself was carried out at room temperature in an ethylene glycol electrolyte containing 170 mM NH_4F (both Sigma-Aldrich, reagent grade) and 1.5 vol.% deionized water. Before the first use, the electrolyte was aged for 9 hours (for details see Ref. 57). The electrochemical cell consisted of a high-voltage potentiostat (PGU-200V, Elektroniklabor GmbH) in a two-electrode configuration, with a Pt foil as counter electrode, and a Ti foil as working electrode. After anodization the Ti foils were rinsed and sonicated in isopropanol and dried in air.

The nanotube Al_2O_3 coating was achieved using an ALD process carried out in a cross-flow process chamber manufactured by FHR Anlagenbau. Trimethylaluminium (TMA, STREM, 98 % purity) and de-ionized water have been evaporated and delivered by bubbling 50 sccm argon carrier gas through stainless steel bubblers at 16°C and 35°C bubbler temperature, respectively. The process chamber temperature was set to 200°C while pressure was kept at 50 Pa, by controlling pumping power by a butterfly valve. The ALD process consisted of 200 cycles at a deposition temperature of 200ºC, with TMA and H_2O as precursors in alternating pulses. Argon was used as carrier and purging gas. The nominal Al_2O_3 coating thickness was 27 nm. The

application of different exposure times of 0.5, 2, 5 and 10 s for the Al precursor (TMA) allowed us to evaluate the influence of the TMA precursor diffusion time on the degree of coating of tube's interior. Due to the higher viscosity of the oxidizing precursor (H_2O) the exposure time was set for 10 s for all processes and it was long enough to attain the saturation of the whole nanotube layer. Purging times for both precursors were set-up long enough (20 s for all processes) to ensure their proper elimination from the ALD chamber and to avoiding any undesirable gas reaction between the precursors.

The QCM measurements were carried out using an Inficon SQM-160 QCM controller and standard 6 MHz AT-cut quartz crystals. Identical TiO_2 nanotube layers (dimensions, aspect ratio) to those subjected to main ALD runs were employed as QCM detector substrates. To prepare stable and robust nanotube-based QCM crystals, free-standing nanotube layers had to be obtained first by dissolution of Ti substrate using Br_2 - MeOH solution.[58] In the next step, the layers were quantitatively transferred and attached on the conventional QCM crystal (14 mm diameter, gold coated, CNT06RCIG, Colnatec) using a small amount of polymeric binder (ethanolic solution containing 9 wt. % of polyvinylpyrrolidone, 2 μl per crystal).

The structural characterization of the TiO_2 nanotube layers before and after ALD runs was carried out by a field-emission scanning electron microscope (FE-SEM JEOL JSM 7500F) and a scanning transmission electron microscope (STEM, FEI Tecnai F20 X-Twin) fitted with high angle annular dark field (HAADF) detector and operating at 200kV. The cross-sectional views were obtained from mechanically bent samples. Due to the rupture of the nanotube layers by this bending, it was possible to visualize nanotubes within the layers and coatings within nanotubes in various directions and nanotube layer depths. These visualizations allowed detailed analyses and measurements of nanotube wall thicknesses and

inner nanotube diameters from the very top to the very bottom. Dimensions of the inner diameters and wall thicknesses of the nanotubes were measured and statistically analyzed by NanoMeasure software. Average values and standard deviations were calculated for all the measurements performed. It turned out from these analyses that the nanotube inner diameter, nanotube wall thickness and nanotube layer depth are strictly related. Hence, the nanotube depth (relevant for the measurement of the Al_2O_3 coating thickness) can be determined from either nanotube wall thickness or inner nanotube diameter values.

Results and Discussion

High aspect ratio (≈180) TiO_2 nanotube layers were fabricated by anodic oxidation of Ti substrates (for details see the Experimental section). The thickness of the nanotube layer was ~20 μm and the inner nanotube diameter at the top of the nanotube layer was ~110 nm. Figure 1a shows a cross-sectional image of the TiO_2 nanotube layer obtained from a mechanically bent TiO_2 nanotube layers introducing the four nanotube depth levels: top, near top, center and bottom. Due to the rupture of the nanotube layer (upon the layer bending) it was possible to image individual nanotubes (and measure their dimensions) at different depths, provided that the absolute depth (from the top of the layer) was very precisely monitored, as described in the experimental part. Figure 1b provides a schematic cross-section of the nanotube structure, with a gradient in the nanotube wall thickness. Due to this gradient, the inner diameter tube decreases from top to the bottom of the nanotube layer so there is a corresponding tube diameter gradient. The unique capabilities of ALD for a uniform deposition of a secondary material into nanotubes, were utilized for the nanotube coating with Al_2O_3 using trimethyl-aluminium (TMA) and H_2O precursors (for further see the Experimental section). In order to evaluate the influence of the

TMA precursor diffusion time on the degree of coating of tube's interior, different TMA exposure times of 0.5, 2, 5 and 10 s were applied. The diffusion time of oxidizing H_2O precursor and purging times for both precursors were kept constant for 10 sec and 20 sec, respectively, throughout the whole work.

Figure 2 shows SEM images of the TiO_2 nanotube layer coated by Al_2O_3, using ALD and 5 seconds TMA exposure time. Figure 2a-d shows Al_2O_3 - coated TiO_2 nanotubes at the different depth levels of the nanotube layers indicated in Figure 1. A further evidence of Al_2O_3 continuous coatings within nanotubes is given in Figure 2e that shows Al_2O_3 coatings protruding out of TiO_2 nanotubes cracked across their wall and in Figure 2f that shows Al_2O_3 coatings embedded within TiO_2 nanotubes cracked along their walls. From all these images it is evident that the Al_2O_3 coating was homogeneous, pinhole-free, and conformal all along the nanotubes.

In addition, analysis of tube layers confirmed the complete coating of the nanotube interiors by Al_2O_3 for all used exposure times. Based on SEM images, Al_2O_3 coating thicknesses, TiO_2 nanotube wall thicknesses, and the TiO_2 nanotube diameters were measured and statistically analyzed by NanoMeasure software. Average values and standard deviations were calculated for all the measurements performed. The nanotube diameter and wall thickness are directly linked with the depth of the nanotube layers. Thus, it was possible to obtain dependence of both values on the depth of the nanotube layers that was with an advantage used in the identification of the actual depth, used in Figure 2.

Based on the SEM visualization and the performed statistical evaluation, two main features can be observed in Figure 2. Firstly, the characteristic nanotube V-shape shown in Figure 1b is clearly reflected on the progressive tube inner diameter, narrowing with an increasing depth of

the nanotubes. Secondly, it is noteworthy that a decreasing thickness of the Al_2O_3 coating was observed at the deepest parts in all the cases studied.

Figure 3a shows the Al_2O_3 coating thickness measured for all the exposure times as a function of both inner nanotube diameter and the nanotube depth, as described in the experimental part. Therein, it can be observed how the coating thickness decreased from nominal value of ≈ 27 nm to lower values at the deepest parts of the nanotubes. In the case of samples with short exposure times (0.5 and 2 s), it is ascribed to an insufficient exposure time of the precursors to coat the deepest levels of the tubes. In principle, in a deposition process beyond the diffusion boundary, a drop of the coating thickness would be noticeable, as it is clearly perceived in Figure 3b-c for short exposure times (0.5 and 2 s). In contrast, the Al_2O_3 coating thickness for long exposure time (5 and 10 s) at the deepest levels of tubes decreases, as it is physically limited within a narrowing inner tube diameter, as a consequence of the tube wall thickness gradient (as shown in Figure 1b). In other words, coating cannot grow thicker as there is no available space for it due to the narrow inner tube diameter. Therefore, the reduction in the Al_2O_3 coating thickness stems from morphological limitations, and not from an insufficient precursor diffusion time as shown in Figure 3d-e, where the Al_2O_3 coating nearly fills the tube interiors leaving a hole with diameter of few nanometers in the coating. Overall, the analysis of the SEM images confirmed the successful homogeneous and conformal coating process of the interior tube surface by a secondary material (Al_2O_3).

In situ QCM measurements were carried out to monitor the ALD process, in particular the variation of the mass increment per cycle. Identical TiO_2 nanotube layers to those layers subjected to main ALD deposition runs (shown in Figures 2 and 3) were employed as QCM detector substrates. This in order to ensure the full compatibility and compliance of the results

obtained from QCM with the results of ALD runs. To carry on QCM measurements without the damage or loss of the nanotube layer, stable and robust nanotube-based QCM crystals were prepared using a tailored route (see Experimental part for details).

Figure 4a shows the QCM results (expressed as the frequency change) from two sets of consecutive ALD cycles registered during two different stages of the Al_2O_3 coating process. The QCM staircase resulted from the alternating TMA and H_2O pulses injected into the deposition chamber during the Al_2O_3 coating process, which took place in discrete steps. Figures 4b and 4c show essentially the same data, but expressed as the mass increase and cumulative mass, respectively, after recalculation using Sauerbrey's equation with standard quartz crystal properties.[59] From these plots it is clear that the QCM measurements displayed the frequency of the mass variation on the sample after each precursor exposure. As in particular evident from Figures 4b and 4c, the major mass gain occurred during the TMA exposure time followed by a slight mass gain after the H_2O exposure period. The slight decrease in mass after the H_2O exposure time has been accounted for recombination of surface hydroxyl groups or desorption of molecular water.[60]

QCM measurements in Figure 4b and 4c show a higher mass uptake during the first stage of the coating process (cycles 11-15) than for a posterior stage (cycles 75-79). The decrease of the deposited mass can be assigned to the reduction of the available surface within the nanotube layer. This is further clear from Figure 4d that shows a normalized comparison of the TMA saturation between ALD cycle 11 and 75. It shows a faster TMA surface saturation at cycle 75 than at cycle 11 and that is a clear proof of reduced surface area. This surface reduction can be described by the following physical scenario. At the initial cycles of the ALD process, the Al_2O_3 coating was deposited both on the exterior and interior TiO_2 nanotube surface. However, a

progressive clogging of the inter-tube space occurred with increasing number of cycles due to the growth of the Al_2O_3 coating, which gradually hampered the diffusion of the precursor molecules towards the exterior surface of the tubes. Once the Al_2O_3 coating clogged the inter-tube space, the deposition processes continued only on the top and within the interior TiO_2 nanotube surfaces, but no longer on the exterior surface. Such reduction of the available surface for Al_2O_3 coating was reflected on a lower uptake mass per cycle (cycles 75-59). The clogged inter-tube space regions by the deposited Al_2O_3 coating were clearly distinguishable as demonstrated in the SEM inset in Figure 4d, where also the Al_2O_3 coating was discerned onto the exterior and interior surface of the nanotubes. The Al_2O_3 coating on the external nanotube surface was very thin. It could not grow thicker due to the clogging of the inter-tube space. Based on the QCM results shown in Figure 4 it also has to be pointed out that the exposure time longer than 10 sec did not have any beneficial effect on the coating of the nanotubes and only led to unnecessary prolongation of the ALD process time.

All these results verified the scenario describing the decreasing mass uptake into the TiO_2 nanotube layer, resulting from the reduction of its available surface, caused by the clogging of the inter-tube space. After the inter-tube clogging had been reached, the frequency per cycle reached a quasi-plateau (cycles 75-79 shown in Figure 4a) related to an exclusive Al_2O_3 coating on the top, and within the interiors of the nanotubes. Using this quasi-plateau process, parameter variations have been carried out to determine the required TMA and H_2O doses, as well as the impact of process temperature and pressure (data not shown here). Overall, these QCM measurements were insightful for the characterization of the Al_2O_3 coating processes carried out within the nanotubes layers by ALD.

In addition, theoretical calculations were performed to determine i) the minimum exposure time to achieve the uniform deposition in the high aspect ratio nanotubes, and ii) to get a deeper understanding on the Al_2O_3 coating process by ALD. We based the theoretical calculations on the work of Elam et al.[56] who used nanoporous anodic alumina membranes as an ideal template for exploring a thin film deposition by ALD into a high aspect ratio structures. They obtained, by Monte Carlo simulations, a mathematical expression that describes the complete and conformal coverage on high aspect ratio nanostructures in the diffusion-limited regime, and provides the minimum exposure time required for such. The mathematical expression described by Elam et al. is as follows:

$$t = 2{,}3 \times 10^{-7}\, P^{-1}\, (m)^{1/2}\, \Gamma\, (L/d)^2 \quad (1)$$

where t is the time in seconds, P is the reactant pressure in Torr, m is the mass of the reactant molecule (TMA) in amu (72), Γ is the density of ALD reactive sites in 10^{15} cm^{-2} (0.2391), d (11 nm) is the tube diameter and L (20 μm) is the nanotube length. The density of reactive sites was calculated from the density of the coating (3.0 g cm^{-3}) and the ALD growth rate. The calculation of the minimum exposure criterion should be estimated from the final aspect ratio of the nanotubes following the complete deposition. In our case, due to the characteristic tube interior diameter gradient, a nanotube layer depth with a diameter of 65 nm was considered, which after a nominal deposition of 27 nm leads to a final tube diameter of 11 nm. The selection of a nanotube layer depth level appropriate to this diameter was not trivial. It had to fulfill two main conditions. Firstly, the selected nanotube layer depth must not have clogged so that the precursor diffusion could continue during the whole deposition process. Secondly, the selected nanotube layer depth should be as deep as possible to preserve the high aspect ratio characteristic of the structure. Nanotube layer depths deeper than the selected one, did not satisfy the first condition as they clogged before the deposition process was completed. No precursor diffusion could take

place there. On the other hand, shallower nanotube layer depths did not fulfill the second condition.

Due to the configuration of the ALD facility, it was not possible to determine the TMA partial pressure value required for the theoretical calculation of the minimum exposure time to obtain uniform coating in the high aspect ratio nanotubes. The precursor TMA was injected into the deposition chamber together with Ar carrier gas, and the total pressure value was known to be 50 Pa. Thus Equation 1, considering the exposure time as a variable, allowed us with an advantage to calculate the TMA partial pressure for different exposure times. TMA partial pressure values for exposure times of 2, 3, 4 and 5 seconds were calculated. It was revealed that the TMA partial pressure values (just below 50 Pa), corresponded to exposure times between 4 and 5 seconds. Shorter exposure times were ruled out as they led to higher TMA partial pressure than the total set pressure (50 Pa). Thus, the calculated exposure times matched coherently with the experimental data shown and discussed in Figure 3-4.

The predicted minimum exposure times are only valid in the diffusion-limited regime i.e., in the limit that $S >> H$, where the reactive sticking coefficient, S, is much greater than the hopping coefficient H. The hopping coefficient value is a function of the aspect ratio of the structure, $H = 16(d/L)^2$, while the reactive sticking coefficient[60] for Al_2O_3 coating by ALD is $S = 1x10^{-3}$. The corresponding hopping coefficient H is $4.84x10^{-6}$ and therefore the condition of $S >> H$ is fulfilled. Thus the predicted minimum exposure time can be considered valid and the diffusion-limited regime can be identified for the presented ALD process in this work.

Finally, in order to assess the quality of the Al_2O_3 coating, scanning transmission electron microscope (STEM) analyses were carried out. Highly uniform, continuous and pinhole-free Al_2O_3 coatings on the inner wall of the TiO_2 nanotube were confirmed by STEM imaging of

individual nanotubes, as shown in Figure 5 that shows a fragment of the nanotube from the upper part (Figure 5a) and from the bottom part (Figure 5b) of the TiO_2 nanotube layer. In particular, the high magnification STEM images of the nanotubes clearly reveal the TiO_2 walls, continuous Al_2O_3 coating on both inner and outer TiO_2 wall, and the gap (pore) in the tube center that can be seen also from SEM images shown as insets (and as essentially demonstrated in Figure 2).

All in all, from all presented results it is clear that ALD with optimized diffusion of precursors can be used for the realization of a range of coatings with different thicknesses and diverse compositions. From this point of view, Al_2O_3 should be only considered as a model material. Many more different materials, such as other oxides, sulfides, nitrides, carbides, etc. can be deposited inside the TiO_2 nanotubes (or virtually any high aspect ratio porous nanostructure) by means of ALD, yielding new functionalities. The results presented here serve as the proof-or-principle that ALD is completely viable tool to prepare uniform coatings within nanotube layers with a thickness, that can be driven by the ALD operator and that stems from the desired application of the coating. It further expands the application portfolio of high aspect ratio TiO_2 nanotubes that were already successfully utilized for water-splitting, photocatalysis, dye-sensitized solar cells, etc.[61-63]

3. Conclusion

In conclusion, an optimization of the ALD coating process of very high aspect-ratio (≈ 180) TiO_2 nanotubular structures by Al_2O_3 was successfully carried out. The influence of the diffusion time of the TMA precursor on the Al_2O_3 coating was studied during the deposition processes. SEM inspection verified that short TMA exposure times (0.5 and 2 seconds) led to inhomogeneous coating. In contrast, a homogeneous coating of the nanotube interior was

achieved by longer TMA exposure times (5 and 10 seconds). The QCM results pointed out on the clogging of the inter-tube space at an early stage of the coating process. This clogging was confirmed by detailed SEM analysis. The inter-tube clogging led to a decrease of the available area and hence to a decrease of the mass uptake, as reflected by the changes within the QCM measurements. Additionally, theoretical exposure minimum time for a complete and uniform coating within the TiO_2 nanotubular layers was calculated. Theoretical and experimental results clearly matched the diffusion-limited regime at the deposition process, and helped to gain important information for the application of the optimum deposition conditions, in high aspect ratio nanotubular structure. Finally, uniform, continuous and pinhole-free Al_2O_3 coating on the inner wall of the TiO_2 nanotubes were confirmed by STEM images. These promising results motivate us to further optimize the ALD process towards coatings or complete inner fillings of even higher aspect ratio nanotube layers with various secondary materials. Such composites nanotube layers could open a promising pathway for further exploration of the exceptional inherent properties of self-organized nanotube TiO_2 layers.

FIGURES

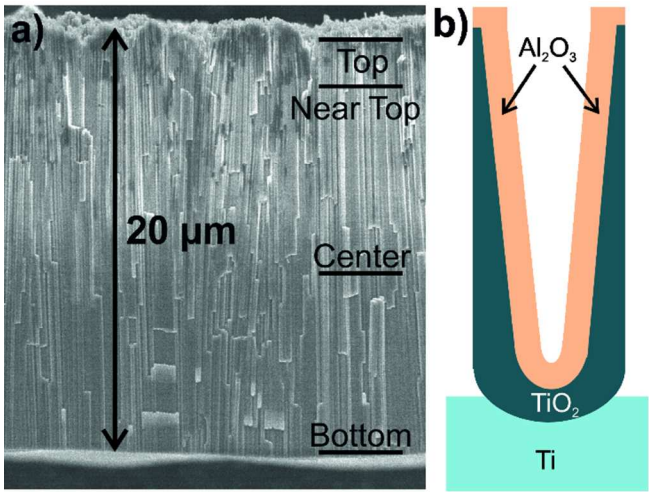

Figure 1. a) cross-sectional SEM image of the 20 μm thick TiO_2 nanotube layer with four different depth levels introduced in this work, b) cross-sectional profile of the nanotubes showing a gradient in the inner tube diameter and the Al_2O_3 coating of the tube interiors.

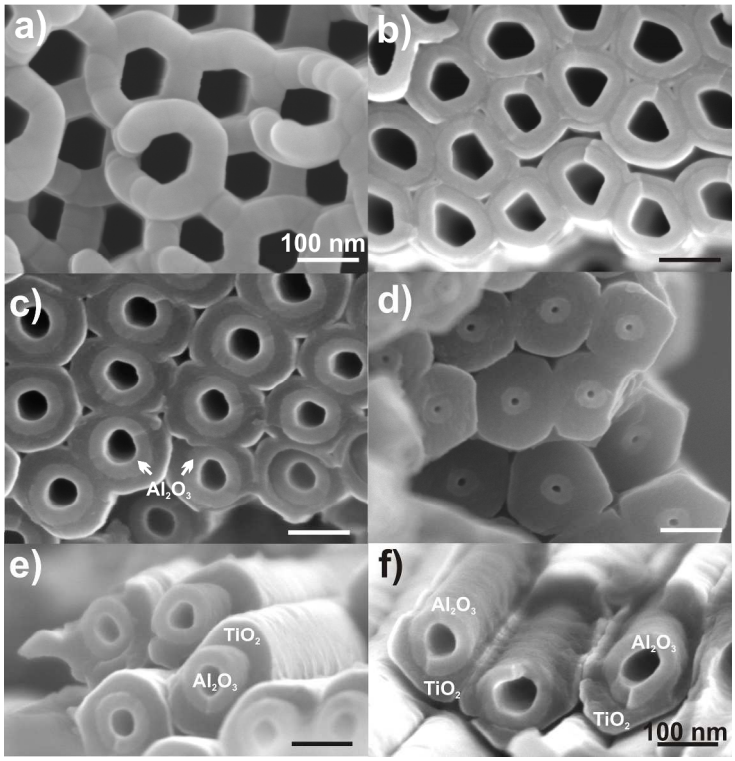

Figure 2. SEM images of TiO_2 nanotubes coated by Al_2O_3 using ALD with 5 seconds TMA exposure time. Images taken at four depth levels: (a) top, (b) near top, (c) center and (d) bottom. Further evidence of Al_2O_3 continuous coatings within nanotubes: (e) Al_2O_3 coatings protruding out of nanotubes cracked across their wall, (f) Al_2O_3 coatings embedded within nanotubes cracked along their walls. The scale bar represents the distance of 100 nm.

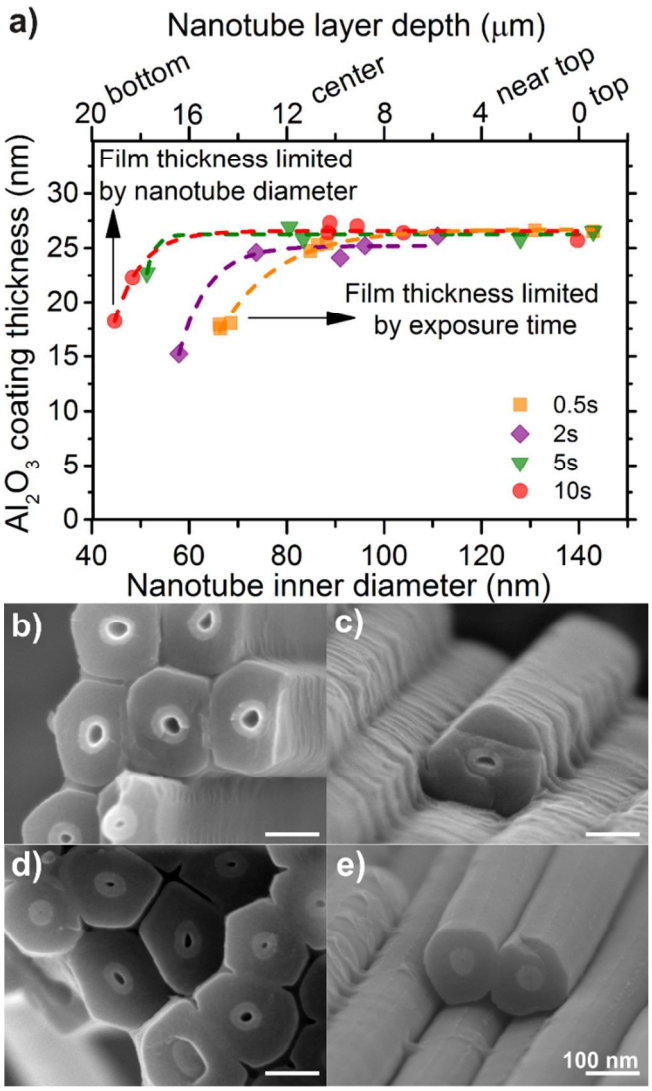

Figure 3. a) Thickness of Al_2O_3 coating (by ALD) as a function of the inner TiO_2 tube diameter and tube depth (0 μm stands for the top part of the tube layer and 20 μm for the bottom part). SEM images taken from nanotube layers for the different TMA exposure times at the tube bottom parts: (b) 0.5 s, (c) 2 s, (d) 5 s and (e) 10 s. The scale bar represents the distance of 100 nm.

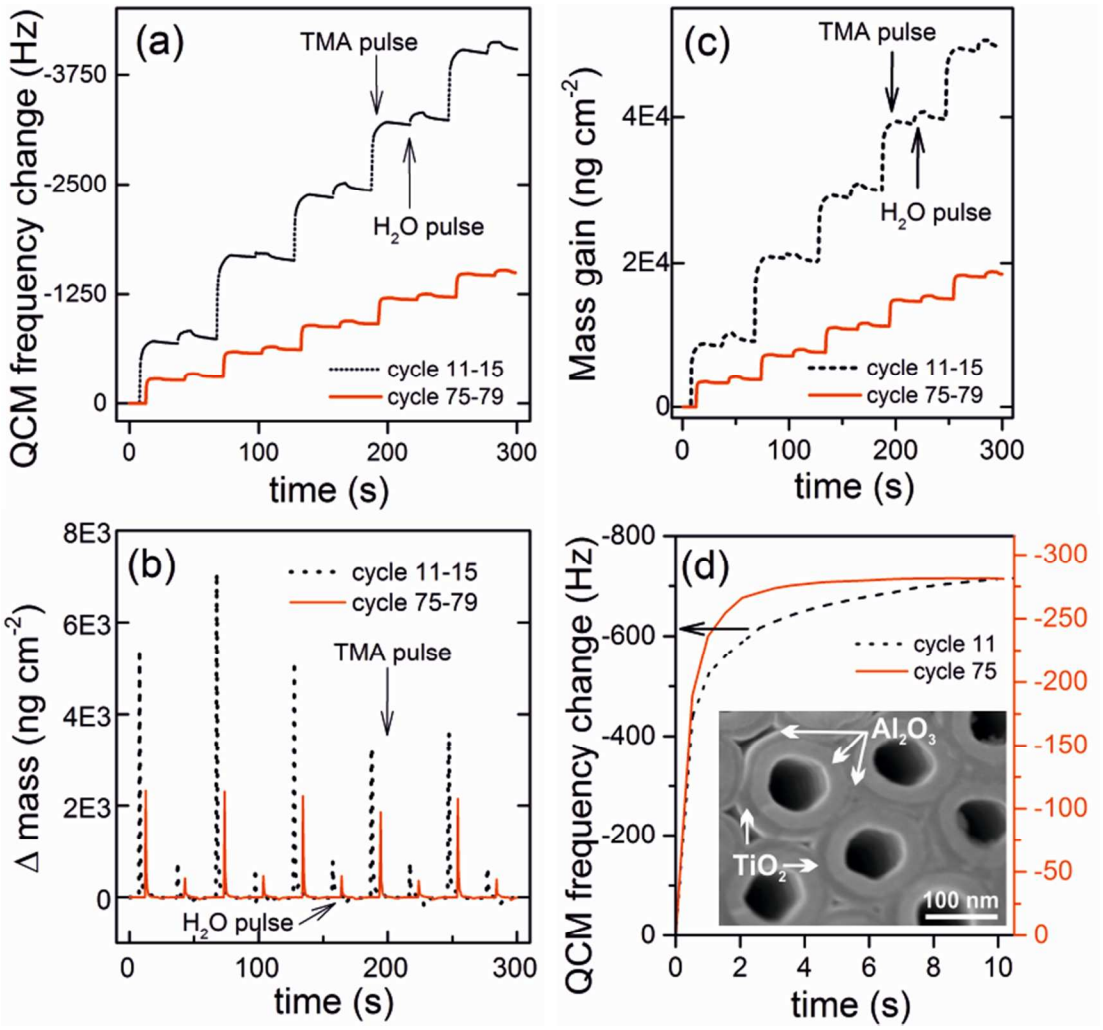

Figure 4. QCM measurements showing the frequency change per cycle as a function of the deposition time, recorded during Al_2O_3 coating of TiO_2 nanotubes layer for 10 seconds TMA exposure time, expressed as (a) the frequency change, (b) the mass increase (c) and cumulative mass uptake that corresponds to the TMA and H_2O exposures (as indicated by arrows), and (d) normalized comparison of TMA saturation curves. For comparison two different stages the coating process (corresponding to specific number of cycles) are shown here. The inset in (d) shows SEM image revealing the clogging of the inter-tube space by the Al_2O_3 coating.

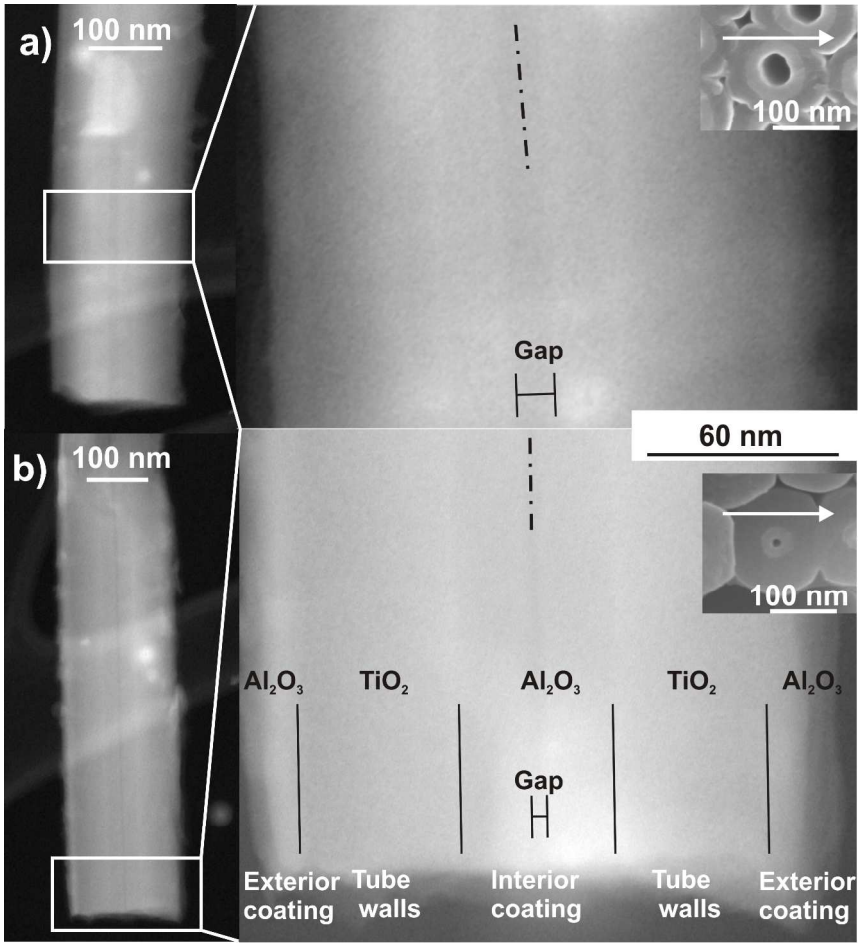

Figure 5. STEM images of fragments of Al_2O_3 coated TiO_2 nanotubes taken from the (a) the upper part and (b) the bottom part of the TiO_2 nanotube layer. The dash-dot lines exhibit the geometrical center axis of the nanotubes. Interfaces between individual parts of the tubes are distinguished by solid lines and appropriate description. Insets show SEM images of corresponding tube parts, where arrows indicate the direction of the STEM imaging through the whole tube.

AUTHOR INFORMATION

Corresponding Author

Jan M. Macak, E-mail: jan.macak@upce.cz

Funding Sources

European Research Council is acknowledged for financial support of this work through project 638857. The authors also thank to Ministery of Youth, Education and Sports of the Czech Republic for financial support via projects CZ.1.05/4.1.00/11.0251, LM2015082 and LM2015087. This work is partly supported by the German Research Foundation (DFG) within the Cluster of Excellence 'Center for Advancing Electronics Dresden' (cfaed).

REFERENCES

(1) Masuda, H.; Fukuda, K. Ordered metal nanohole arrays made by a two-step replication of honeycomb structures of anodic alumina. *Science*, **1995**, *268*, 1466.

(2) Masuda, H.; Fukuda, K. Highly ordered nanochannel-array architecture in anodic alumina. *Appl. Phys. Lett*. **1997**, *71*, 2770.

(3) Zwilling, V.; Aucouturier, M; Darque-Ceretti, E. Anodic oxidation of titanium and TA6V alloy in chromic media. An electrochemical approach. *Electrochim. Acta*, **1999**, *45*, 921.

(4) D. Gong, D.;Grimes, C. A.; Varghese, O. K.; Chen, Z; Dickey, E.C. Titanium oxide nanotube arrays prepared by anodic oxidation, *J. Mater. Res*. **2001**, *16*, 3334.

(5) Beranek, R.; Hildebrand, H.; Schmuki, P. Self-organized porous titanium oxide prepared in H_2SO_4 / HF electrolytes. *Electrochem. and Solid-St. Lett*. **2003**, *6*, B12.

(6) Macak, J. M.; Sirotna, K.; Schmuki, P. Self-organized porous titanium oxide prepared in Na_2SO_4/NaF electrolytes. *Electrochim. Acta*, **2005**, *50*, 3679.

(7) Al Mawiawi, D.; Coombs, N.; Moskovits, M. Magnetic properties of Fe deposited into anodic aluminum oxide pores as a function of particle size. *J. App. Phys*. **1991**, *70*, 4421.

(8) Masuda, H.; Yotsuya, M.; Asano. M.; Kazuyuki, N.; Nakao, M.; Yokoo, A.; Tamamura, T. Self-repair of ordered pattern of nanometer dimensions based on self-compensation properties of anodic porous alumina. *Appl. Phys. Lett.* **2001**, *78*, 826.

(9) Jeong, S.-H.; Hwang, H.-Y.; Lee, K.-H.; Jeong, Y. Template-based carbon nanotubes and their application to a field emitter. *Appl. Phys. Lett.* **2001**, 7*8*, 2052.

(10) Bae, C.; Yoo, H.; Kim, S.; Lee, K.; Kim, J.; Sung, M. M.; Shin, H. Template-directed synthesis of oxide nanotubes: fabrication, characterization, and applications. *Chem. Mater*. **2008**, *20*, 756.

(11) Wang, Y.; Lee, J. Y.; Zeng, H. C. Polycrystalline SnO_2 nanotubes prepared via infiltration casting of nanocrystallites and their electrochemical application. *Chem. Mater*. **2005**, *17*, 3899.

(12) Du, N.; Zhang, H.; Chen, B. D.; Wu, J. B.; Ma, X. Y.; Liu, Z. H.; Y. Q. Zhang, D. R. Yang, X. H. Huang, J. P. Tu, Porous Co_3O_4 Nanotubes derived from $Co_4(CO)_{12}$ clusters on carbon nanotube templates: a highly efficient material for Li-battery applications. *Adv.Mater*. **2007**, *19*, 4505.

(13) Macak, J. M.; Tsuchiya, H.; Ghicov, A.; Yasuda, K.; Hahn, R.; Bauer, S.; Schmuki, P. TiO_2 nanotubes: Self-organized electrochemical formation, properties and applications. *Curr. Opin. Solid State Mater. Sci*. **2007**, *11*, 3.

(14) Roy, P.; Berger, S.; Schmuki, P. TiO_2 nanotubes: Synthesis and applications. *Angew. Chem. Int. Ed.* **2011**, *50*, 2904.

(15) Lee, K.; Mazare, A.; Schmuki, P. One-dimensional titanium dioxide nanomaterials: nanotubes. *Chem. Rev.* **2014**, *114*, 9385.

(16) Macak, J. M.; Tsuchiya, H.; Schmuki, P. High-aspect-ratio TiO_2 nanotubes by anodization of titanium. *Angew. Chem. Int. Ed.* **2005**, *44,* 2100.

(17) Macak, J. M.; Tsuchiya, H.; Taveira, L.; Aldabergerova, S.; Schmuki, P. Smooth anodic TiO_2 nanotubes. *Angew. Chem. Int. Ed*. **2005**, *44*, 7463.

(18) Albu, S. P.; Ghicov, A.; Macak, J. M.; Schmuki, P. 250 μm long anodic TiO_2 nanotubes with hexagonal self-ordering. *Phys. Stat. Sol. (RRL)*, **2007**, *1*, R65.

(19) Macak, J. M.; Albu, S.; Schmuki, P. Towards ideal hexagonal self-ordering of TiO_2 nanotubes. *Phys. Stat. Sol. (RRL)*, **2007**, *1*, 181.

(20) Zhu, K.; Neale, N.; Miedaner, A.; Frank, A. Enhanced charge-collection efficiencies and light scattering in dye-sensitized solar cells using oriented TiO_2 nanotubes arrays. *Nano Lett.* **2007**, *7*, 69.

(21) Wang, D.; Yu, B.; Wang, C.; Zhou, F.; Liu, W. A novel protocol toward perfect alignment of anodized TiO_2 nanotubes. *Adv. Mater*. **2009**, *21,* 1964.

(22) Lu, K.; Tian, Z.; Geldmeier, J. A. Polishing effect on anodic titania nanotube formation. *Electrochim. Acta*, **2011**, *56*, 6014.

(23) Kondo, T.; Nagao, S.; Yanagishita, T.; Nguyen, N.T.; Lee, K.; Schmuki, P.; Masuda, H. Ideally ordered porous TiO_2 prepared by anodization of pretextured Ti by nanoimprinting process. *Electrochem. Commun*. **2015**, *50*, 73

(24) Sopha, H.; Jäger, A.; Knotek, P.; Tesar, K.; Jarosova, M.; Macak, J.M. Self-organized Anodic TiO_2 Nanotube Layers: Influence of the Ti substrate on Nanotube Growth and Dimensions. *Electrochim. Acta*, **2016**, *190*, 744.

(25) Mirabolghasemi, H.; Liu, N.; Lee, K.; Schmuki, P. Formation of 'single walled' TiO_2 nanotubes with significantly enhanced electronic properties for higher efficiency dye-sensitized solar cells. *Chem. Commun*. **2013**, *49*, 2067.

(26) Zhu, K.; Neale, N. R.; Helverson, A. F.; Kim, J. Y.; Frank, A. J. Effects of Annealing Temperature on the Charge-Collection and Light-Harvesting Properties of TiO_2 Nanotube-Based Dye-Sensitized Solar Cells. *J. Phys. Chem. C*, **2010**, *114*, 13433.

(27) Ghicov, A.; Tsuchiya, H.; Macak, J. M.; Schmuki, P. Annealing effects on the photoresponse of TiO_2 nanotubes. *Phys. Stat. Sol. (RRL)*, **2006**, *203*, R28.

(28) Wang, D.; Liu,L.; Zhang, F.; Tao, K.; Pippel, E.; Domen K., Spontaneous phase and morphology transformation of anodized titania nanotubes induced by water at room temperature. *Nano Lett.*, **2011**, *11*, 3649-3655.

(29) Liao, Y.; Que, W.; Zhong, P.; Zhang, J.; He, Y., A facile method to crystallize amorphous anodized TiO_2 nanotubes at low temperature. *ACS Appl. Mater. Interfaces*, **2011**, *3*, 2800-2804.

(30) Paulose, M.; Shankar, K.; Varghese, O. K.; Mor, G. K; Grimes, C. A. Application of highly-ordered TiO_2 nanotube-arrays in heterojunction dye-sensitized solar cells. *J. Phys. D: Appl. Phys*. **2006**, *39*, 2498.

(31) Sadek, A. Z.; Zheng, H.; Latham, K.; Wlodarski, W.; Kalantar-zadeh, K. Anodization of Ti thin film deposited on ITO. *Langmuir*, **2009**, *25*, 509.

(32) Kathirvel, S.; Su, C.; Yang, C.-Y.; Shiao, Y.-J.; Chen, B.-R.; Li, W.-R. The growth of TiO_2 nanotubes from sputter-deposited Ti film on transparent conducting glass for photovoltaic applications. *Vacuum*, **2015**, *118*, 17.

(33) Macak, J. M.; Gong, B. G.; Hueppe, M.; Schmuki, P. Filling of TiO_2 nanotubes by self-doping and electrodeposition. *Adv. Mater*. **2007**, *19*, 3027.

(34) Macak, J. M.; Zollfrank, C.; Rodriguez, B. J.; Tsuchiya, H.; Alexe, M.; Greil, P.; Schmuki, P. Ordered ferroelectric lead titanate nanocellular structure by conversion of anodic TiO_2 nanotubes. *Adv. Mater.* **2009**, *21*, 3121.

(35) Assaud, L.; Heresanu, V.; Hanbücken, M.; Santinacci, L. Fabrication of p/n heterojunctions by electrochemical deposition of Cu_2O onto TiO_2 nanotubes. *C.R.Chimie*, **2013**, *16*, 89

(36) Fang, D.; Huang, K.; Liu, S.; Qin, D.; High density copper nanowire array deposition inside ordered titania pores by electrodeposition. *Electrochem. Commun*., **2009**, *11*, 901-904.

(37) Sun, W.-T.; Yum, Y.; Pan, H.-Y.; Gao, X.-F.; Chen, Q.; Peng, L.-M. CdS quantum dots sensitized TiO_2 nanotube-array photoelectrodes. *J. Am. Chem. Soc*., **2008**, *130*, 1124.

(38) Baker, D. R.; Kamat, P. Photosensitization of TiO_2 nanostructures with CdS quantum dots: Particulate versus tubular support architectures. *Adv. Func. Mater*. **2009**, *19*, 805.

(39) Sun, W.-T.; Yu, Y.; Pan, H-Y.; Gao, X.-F.; Chen, Q.; Peng, L.-M., CdS quantum dots sensitized TiO_2 nanotube-array photoelectrodes. *J. Am. Chem. Soc.*, **2008**, *130*, 1124-1125

(40) Wang, G.; Qiao, J.; Gao, S., Fabrication of $Zn_xIn_{1-x}S$ quantum dot-sensitized TiO_2 nanotube arrays and their photoelectrochemical properties. *Mater. Lett.*, **2014**, *131*, 354-357

(41) Macak, J. M.; Kohoutek, T.; Wang, L.; Beranek, R. Fast and robust infiltration of functional material inside titania nanotube layers: case study of a chalcogenide glass sensitizer. *Nanoscale*, **2013**, *5*, 9541.

(42) Ju, S. H.; Han, S.; Kim, J. S. The growth and morphology of copper phthalocyanine on TiO_2 nanotube arrays. *J. Ind. Eng. Chem*. **2013**, *19*, 272.

(43) Yoo, J. E.; Lee, K.; Altomare, M.; Selli, E.; Schmuki, P. Self-organized arrays of single-metal catalyst particles in TiO_2 cavities: A highly efficient photocatalytic system. *Angew. Chem. Int. Ed.* **2013**, *52*, 7514.

(44) Nguyen, N. T.; Yoo, J. E.; Altomare, M.; Schmuki, P. ‘‘Suspended’’ Pt nanoparticles over TiO_2 nanotubes for enhanced photocatalytic H_2 evolution. *Chem. Commun*. **2014**, *50*, 9653.

(45) Yoo, J. E.; Lee, K.; Schmuki, P. Templating using self-Aligned TiO_2 nanotube stumps: Highly ordered metal and polymer bumped arrays. *ChemElectroChem*, **2014**, *1*, 64.

(46) Sarkar, S. K.; Kim, J. Y.; Goldstein, D. N.; Neale, N. R.; Zhu, K.; Elliott, C. M.; Frank, A. J.; George, S. M. In_2S_3 atomic layer deposition and its application as a sensitizer on TiO_2 nanotube arrays for solar energy conversion. *J. Phys. Chem. C*, **2010**, *114*, 8032.

(47) Tupala, J.; Kemell, M.; Härkönen, E.; Ritala M.; Leskelä., M. Preparation of regularly structured nanotubular TiO_2 thin films on ITO and their modification with thin ALD-grown layers. *Nanotechnology*, **2012**, *23*, 125707.

(48) I. Turkevych, S. Kosar, Y. Pihosh, K. Mawatari, T. Kitamori, J. Ye, K. Shimamura. Synergistic effect between TiO_2 and ubiquitous metal oxides on photocatalytic activity of composite nanostructures. *J. Ceram. Soc. Jap*. **2014**, *122*, 393.

(49) Assaud, L.; Brazeau, N.; Barr, M.K.S.; Hanbuecken, M.; Ntais, S.; Baranova, E.A.; Santinacci, L., Atomic layer deposition of Pd nanoparticles on TiO_2 nanotubes for ethanol electrooxidation: synthesis and electrochemical properties. *ACS Appl. Mater. Interfaces*, **2015**, *7*, 24533–24542.

(50) Macak, J. M. Self-organized Anodic TiO_2 Nanotubes: Functionalities and Applications Due to a Secondary Material. In *Electrochemically Engineered Nanoporous Structures*; Losic, D; Santos, A. Springer International Publishing, Switzerland, 2015.

(51) Macak, J. M.; Prikryl, J.; Sopha, H.; Strizik, L. Antireflection ln_2O_3 coatings of self-organized TiO_2 nanotube layers prepared by atomic layer deposition. *Phys. Stat. Sol. (RRL)*, **2015**, *9*, 516.

(52) Gui, Q.; Zhen, X.; Zhang, H.; Cheng, C.; Zhu, X.; Yin, M.; Song, Y.; Lu, L.; Chen, X.; Li, D. Enhanced photoelectrochemical water splitting performance of anodic TiO_2 nanotube arrays by surface passivation. *ACS Appl. Mater. Interfaces,* 2014, *6 (19)*, 17053.

(53) Jae-Yup, K.; Kyeong-Hwan, L.; Junyoung, S.; Sun Ha, P.; Jin Soo, K.; Kyu Seok, H.; Myung Mo, S.; Nicola, P.; Yung-Eun, S. Highly ordered and vertically oriented TiO_2/Al_2O_3 nanotube electrodes for application in dye-sensitized solar cells, *Nanotechnology,* **2014**, *25 (50)*, 504003.

(54) Detavernier, C.; Dendooven, J.; Sree, S.P.; Ludwig, K.F.; Marents, J.A., Tailoring nanoporous materials by atomic layer deposition. *Chem. Soc. Rev.*, **2011**, *40*, 5242-5253.

(55) Wu, Y.; Assaud, L.; Kryschi, C.; Capon, B.; Detavernier, Ch.; Santinacci, L.; Bachmann, J., Antimony sulfide as a light absorber in highly ordered, coaxial nanocylindrical arrays: preparation and integration into a photovoltaic device. *J. Mater. Chem. A*, **2015**, *3*, 5971-5981.

(56) Elam, J. W.; Routkevitch, D.; Mardilovich, P. P.; George, S. M. Conformal coating on ultrahigh-aspect-ratio nanopores of anodic alumina by atomic layer deposition. *Chem. Mater*. **2003**, *15*, 3507.

(57) Sopha, H.; Hromadko, L.; Nechvilova, K.; Macak, J. M. Effect of electrolyte age and potential changes on the morphology of TiO_2 nanotubes. *J. Electroanal. Chem*., **2015**, *759*, 122.

(58) Albu, S.; Ghicov, A.; Macak, J.M.; Hahn, R.; Schmuki, P. Self-Organized, Free-Standing TiO_2 Nanotube Membrane for Flow-through Photocatalytic Applications. *Nano. Lett*. **2007**, *7*, 1286.

(59) Sauerbrey, G. Verwendung von Schwingquarzen zur Wägung dünner Schichten und zur Mikrowägung, *Z. Physik*, 1959, **155**, 206.

(60) Elam, J. W.; Groner, M. D.; George, S. M. Viscous flow reactor with quartz crystal microbalance for thin film growth by atomic layer deposition. *Rev. Sci. Instrum*. **2002**, *73*, 2981.

(61) Basahel, S.N.; Lee, K.; Hahn, R.; Schmuki, P.; Bawaked, S. M.; Al-Thabaiti, S. A. Self-decoration of Pt metal particles on TiO_2 nanotubes used for highly efficient photocatalytic H_2 production. *Chem. Commun.* **2014**, *50*, 6123.

(62) Liu, N.; Paramasivam, I.; Yang, M.; Schmuki, P. Some critical factors for photocatalysis on self-organized TiO_2 nanotubes. *J. Solid State Electrochem.* **2012**, *16*, 3499.

(63) So, S.; Hwang, I.; Schmuki, P. Hierarchical DSSC structures based on "single walled" TiO_2 nanotube arrays reach a back-side illumination solar light conversion efficiency of 8%. *Energy Environ. Sci.* **2015**, *8*, 849.

Table of contents

Uniform coating of high aspect ratio TiO_2 nanotube layers (AR ≈180) by a secondary material (Al_2O_3) using atomic layer deposition is presented here. The coating uniformity was verified by SEM images and it was found perfect even at the deepest nanotube parts.

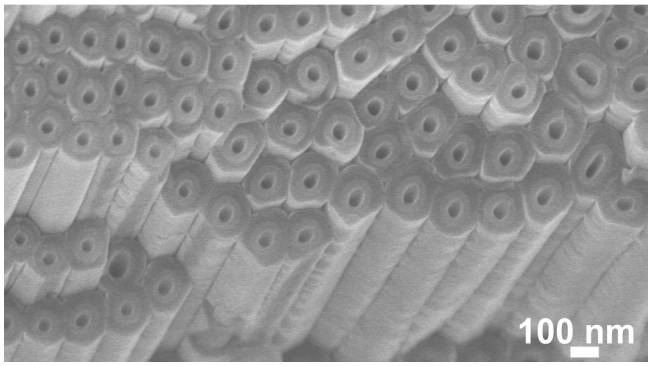

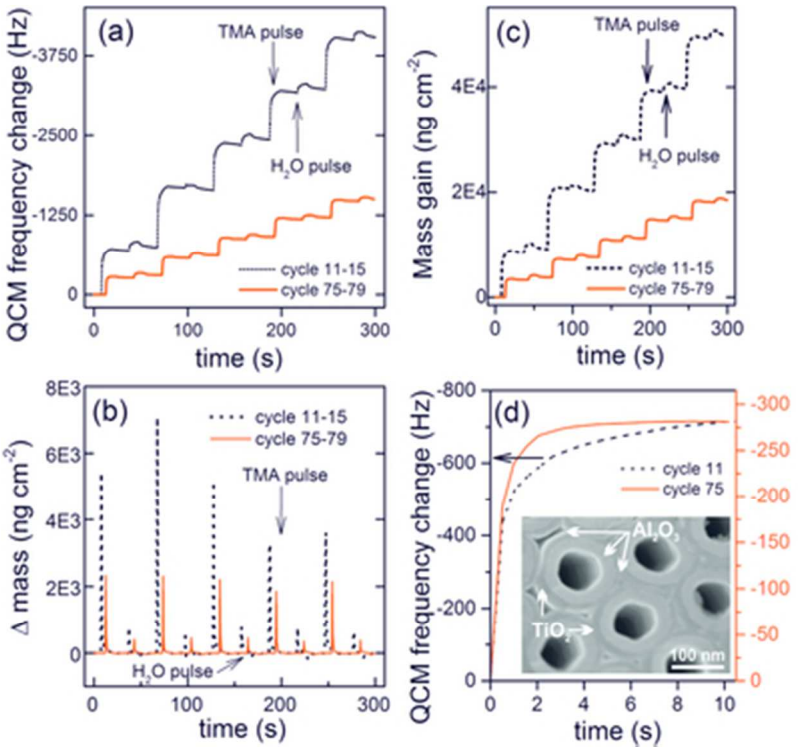

Figure 4. QCM measurements showing the frequency change per cycle as a function of the deposition time, recorded during Al2O3 coating of TiO2 nanotubes layer for 10 seconds TMA exposure time, expressed as (a) the frequency change, (b) the mass increase (c) and cumulative mass uptake that corresponds to the TMA and H2O exposures (as indicated by arrows), and (d) normalized comparison of TMA saturation curves. For comparison two different stages the coating process (corresponding to specific number of cycles) are shown here. The inset in (d) shows SEM image revealing the clogging of the inter-tube space by the Al2O3 coating.

33x31mm (300 x 300 DPI)

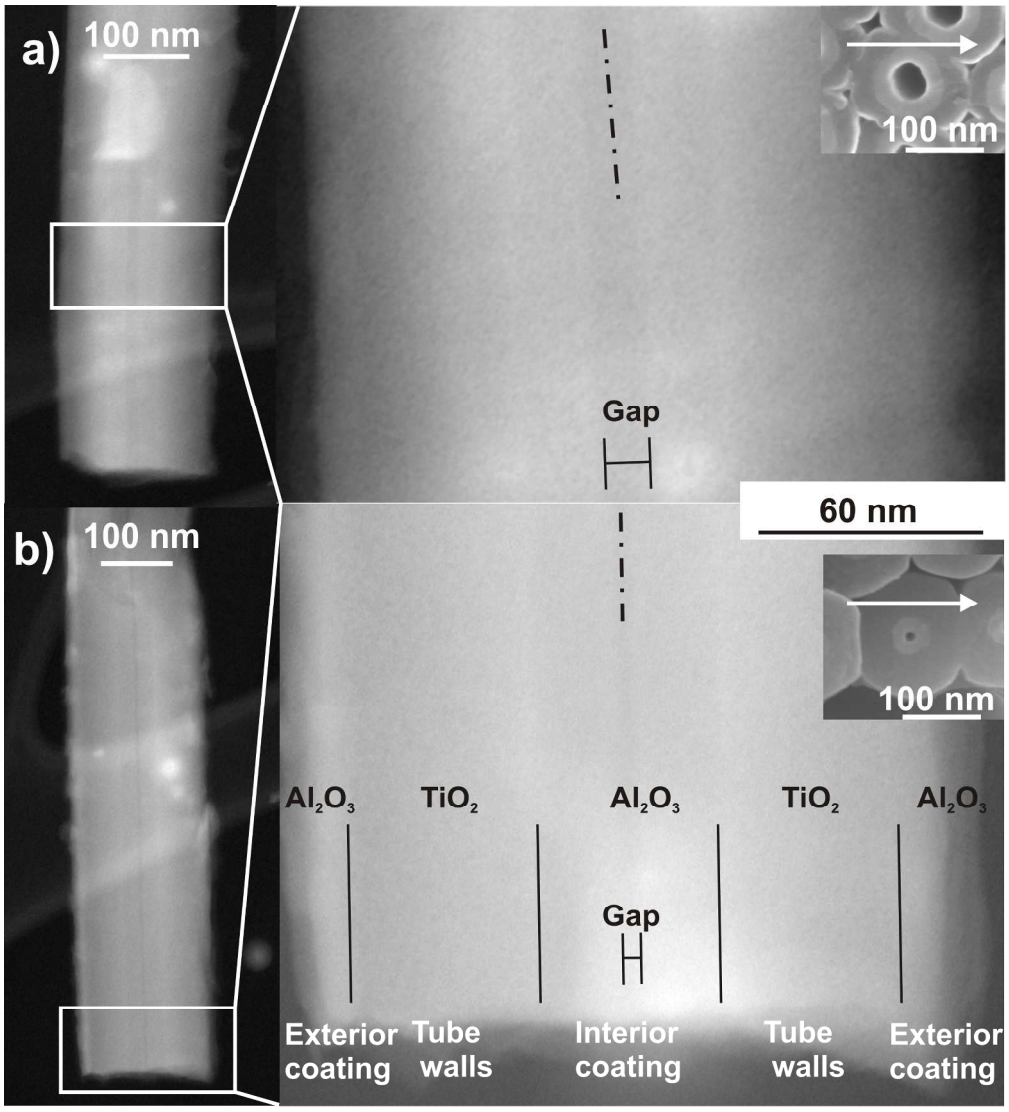

Figure 5. STEM images of fragments of Al2O3 coated TiO2 nanotubes taken from the (a) the upper part and (b) the bottom part of the TiO2 nanotube layer. The dash-dot lines exhibit the geometrical center axis of the nanotubes. Interfaces between individual parts of the tubes are distinguished by solid lines and appropriate description. Insets show SEM images of corresponding tube parts, where arrows indicate the direction of the STEM imaging through the whole tube.